Mechanics of Advanced Composite Structures 8 (2021) 401-414

Mechanics of Advanced Composite Structures

journal homepage: http://MACS.journals.semnan.ac.ir

Semnan University

Vibration in an Electrically Affected Hygro-magneto-thermo-flexo Electric Nanobeam Embedded in Winkler-Pasternak Foundation

R. Selvamani[a*], J. Rexy[b], F. Ebrahimi[c]

[a] *Department of Mathematics, Karunya Institute of Technology and Sciences, Coimbatore-641114, Tamilnadu, India.*
[b] *Department of Mathematics, Karunya Institute of Technology and Sciences, Coimbatore, 641114, India.*
[c] *Department of Mechanical Engineering, Imam Khomeini International University Qazvin, Iran*

KEYWORDS

Applied voltage
Hygro thermomagnetic effect
Flexoelectric nanobeam
Nonlocal elasticity theory
Refined beam theory

ABSTRACT

This paper presents applied electric voltage performance in hydrothermal magneto flexo electric nanobeams embedded in the Winkler-Pasternak foundation based on nonlocal elasticity theory. Higher-order refined beam theory via Hamilton's principle is utilized to arrive at the governing equations of nonlocal nanobeams and solved by implementing an analytical solution. A parametric study is presented to analyze the effect of the applied electric voltage on dimensionless deflection via nonlocal parameters, slenderness, moisture constant, critical temperature, and foundation constants. It is found that physical variants and beam geometrical parameters significantly affect the dimensionless deflection of nanoscale beams. The accuracy and efficiency of the presented model are verified by comparing the results with that of published researches. A good agreement has arrived. The numerical examples are presented to explain how each variant can affect the structure's stability endurance. This type of model and its physical output show the great potential of hygro-magneto-thermo-flexo electric combination in the design of intelligent composite structures and use in structural health scanners. Recent advances in the application of nanotechnology have resulted in the manufacture of nanoelectromechanical devices. The attractiveness of them is due to their excellent and distinctive mechanical and electrical properties.

1. Introduction

Structural monitoring of electrical nanobeams, nanoplates, and nanomembranes is a recent novel field for many researchers due to their quality properties. The classical continuum theory is applied practically in the mechanical behavior of macroscopic structures. Still, it is improperly for the size effect on the mechanical treatments on micro- or nanoscale structure. Nevertheless, the classical continuum theory needs to be extended to factor in the nanoscale results. The prime magneto-electro-elastic (MEE) was used in the 1970s, and the MEE composite consisting of the piezoelectric and piezo magnetic phases was discovered this year. Van Den Boomgard et al. [1] the MEE nanomaterials (BiFeO3, BiTiO3-CoFe2O4, NiFe2O4-PZT) and their nanostructures became a significant role in researches (Zheng et al. [2], Martin et al. [3], Wang et al. [4], Prashanthi et al. [5]). For this reason, nanostructure's major potential for amplification many applications, their mechanical behavior should be investigated and well-identified before new designs can be proposed. The classical mechanic continuum theories demonstrate that to predict the response of structures up to a minimum size sub, they fail to provide accurate predictions. The nonlocal theories add a size parameter in the modeling of the continuum. This paper studied models that developed according to the greatly used nonlocal elasticity theory (Eringen [6], Eringen [7], Eringen [8], Eringen [9]). Timoshenko beam theory nonlocal elasticity was investigated in their study. So based on an elastic medium, the stability response of SWCNT is described. Winkler and Pasternak parameters, the aspect ratio of the SWCNT, and the nonlocal parameter were studied. Nonlinear free vibration of SWCNTs based on Eringen's nonlocal elasticity theory was developed by Yang et al. [10]. Ehyaei and Akbarizadeh [11] discussed vibration analysis of the micro composite thin beam based on modified couple stress theory elaborately.

* Corresponding author. Tel.: +98-91-24396001; Fax: +98-61-42426666
Email address: vnorouzi@jsu.ac.ir

DOI: 10.22075/MACS.2021.22068.1311
Received 20-12-10; Received in revised form 21-06-04; Accepted 21-11-15

Later, Ebrahimi and Barati [12] developed a unified formulation to model inhomogeneous nonlocal beams. Free vibration analysis of chiral double-walled carbon nanotube embedded in an elastic medium using nonlocal elasticity theory and Dihaj et al. [13] have investigated Euler- Bernoulli beam model. The vibration and buckling of piezoelectric and piezomagnetic nanobeams are verified based on the third-order beam model by Ebrahimi and Barati [14, 15, 16, 17]. The vibration, buckling, and bending of Timoshenko nanobeams based on a meshless method was proposed by Roque et al. [18]. Embedded in the nonlocal component relevance of Eringen, major articles were published searching to enlarge nonlocal beam models for nanostructures Peddieson et al. [19]. A novel method was proposed via nonlocal Euler–Bernoulli and Timoshenko beam theory, accepted by many studies to verify bending of the beam by (Civalek and Demir [20], Wang [21], Wang et al. [22]). During the years of research the small-size agents in SWCNTs, several studies were devoted by (Murmu and Pradhan [23], Karami et al. [24]) for the wave propagation of functionally graded anisotropic nanoplates resting on the Winkler-Pasternak foundation. The propagation of elastic waves in thermally affected embedded carbon-nanotube-reinforced composite beams via various shear deformation plate theories was analyzed by Ebrahimi and Rostami [25].

Hajnayeb and Foruzande [26] verify free vibration analysis of a piezoelectric nanobeam using nonlocal elasticity theory with its numerical computation. Thermo-magneto-electro vibrations of FG nanobeam and plates are studied for stability analysis via various physical variants by Ebrahimi et al. [27], Ebrahimi et al. [28], Ebrahimi et al. [29]. Yazdi has discussed the large amplitude forced vibration of the functionally graded nanocomposite plate with piezoelectric layers resting on a nonlinear elastic foundation [30]. Thermo-magneto-electro-elastic analysis of a functionally graded nanobeam integrated with functionally graded piezomagnetic layers was proposed in composite structures by Arefi and Zenkour [31]. An investigation has been conducted on the wave propagation analysis of smart strain gradient piezo-magneto-elastic nonlocal beams by Ebrahimi and Barati [32]. The static analysis of laminated piezo-magnetic size-dependent curved beam was concentrated on the modified couple stress theory by Arefi [33]. Studies were conducted on the analytical solutions to magneto-electro-elastic beams by Aimin and Haojiang [34].

Furthermore, many researchers have presented the static and dynamic characteristics of beams and plates exposed to hygro-thermal environments because of the considerable effects on the structure's behavior. An analytical method to determine Gayen and Roy [35] presented the stress distributions in circular tapered laminated composite beams under hygro and thermal loadings in detail. Kurtinaitiene et al. [36] introduced the effect of additives on the hydrothermal synthesis of manganese ferrite nanoparticles. The size effects on static behavior of nanoplates resting on elastic foundation subjected to hygro-thermal loadings have been developed using several beam theories by Alzahrani et al. [37]. They extended the nonlocal constitutive relations of Eringen to contain the hygro-thermal effects. Also, Sobhy [38] studies show the frequency response of simply-supported shear deformable orthotropic graphene sheets exposed to hygro-thermal loading.

Ghorbanpour Arani and Zamani [39] examined the bending of electro-mechanical sandwich nanoplate based on silica aerogel foundation with physical variables. They described that the influence of parameters on nanostructures such as applied voltage, porosity index, foundation characteristics, parameter, plate aspect ratio, and thickness ratio was studied on bending response of sandwich nanoplate. It was shown that the three-unknown shear and normal deformations nonlocal beam theory for the bending analysis by Simsek et al. [40]. He researched the bending and buckling of the FG based on the nonlocal Timoshenko and Euler–Bernoulli beam theory. Also, he was described that the power-law exponent has a wide influence on the responses of FG nanobeam. Free vibration of size-dependent magneto-electro-elastic nanoplates was derived by authors (Ke et al. [41], Ramirez et al. [42]).

Authors, Zur et al. [43], Arefi et al. [44], Arefi and Zenkour [45], Arefi and Zenkour [46], Arefi et al. [47] have investigated free vibration and bending analyses of thermo-magneto-electro-elastic of nanoplates. Arefi and Zenkour [48] studied the size-dependent electro-elastic analysis of a sandwich microbeam based on higher-order sinusoidal shear deformation theory and strain gradient theory. Arefi and Rabczuk [49] analyzed the nonlocal higher-order shear deformation theory for electro-elastic analysis of a piezoelectric doubly curved nanoshell. They concluded that with an increase of nonlocal parameters, the stiffness of the nanoshell is decreased. Consequently, the displacement components, rotation component, and maximum electric potential are increased significantly. Barati et al. [50] reported the dynamic response of nanobeams subjected to moving nanoparticles and hygro-thermal environments based on nonlocal strain gradient theory. They found that the dynamic deflection increased as the temperature/moisture increased. Bending vibration and electro-magneto-elastic responses of piezomagnetic curved nanobeams have been developed by authors Arefi and Zenkour [51, 52]). Zenkour and Alghanmi [53] constructed the analytical model for the static response of sandwich plates with FG core and piezoelectric faces under thermo-electro-mechanical loads and resting on elastic foundations. They have shown that the inclusion of Pasternak's foundation reduces deflections. The modified coupled stress theory and vibration analysis of nanobeams resting on visco-Pasternak foundations have been studied by Sobhy and Zenkour [54] and Zenkour and El-Shahrany [55].

Barati and Zenkour [56] analyzed the forced vibration of sinusoidal FG nanobeams resting on hybrid Kerr foundation in hygro-thermal environments. They also found that increase of Kerr foundation parameters leads to postponement in resonance frequencies of FG nanobeams. Daik and Zenkour [57] reported the bending of Functionally Graded Sandwich Nanoplates Resting on Pasternak Foundation under Different Boundary Conditions. The electro-mechanical energy absorption, resonance frequency, and low-velocity impact analysis of the piezoelectric doubly curved system were derived by Guo et al. [58]. Dai et al. [59] developed on the vibrations of the non-polynomial viscoelastic composite open-type shell under residual stresses. Dynamic simulation of the ultra-fast-rotating sandwich cantilever disk via finite element is modeled by Wu and Habibi [60]. Al-Furjan et al. [61] introduced the vibrational characteristics of a higher-order laminated composite viscoelastic annular microplate via modified couple stress theory. Al-Furjan et al. [62] proposed the three-dimensional frequency response of the CNT-Carbon-Fiber reinforced laminated circular/annular plates under initial stresses. Non-polynomial framework for stress and strain response of the FG-GPLRC disk using three-dimensional refined higher-order theory was derived by Al-Furjan et al. [63]. Dai et al. [64] investigated the frequency characteristics and sensitivity analysis of a size-dependent laminated nanoshell.

Wang et al. [65] developed the frequency and buckling responses of a high-speed rotating fiber metal laminated cantilevered microdisk. Ghabussi et al. [66] constructed the seismic performance assessment of a novel ductile steel braced frame equipped with Steel curved dampers. Ghabussi et al. [67] proposed the frequency characteristics of a viscoelastic graphene nanoplatelet–reinforced composite circular microplate. Ghabussi et al. [68] studied the improving seismic performance of portal frame structures with steel curved dampers. They observed that there were significant improvements in the seismic performance of both types of portal frames by utilizing proposed steel curved dampers. Zhao et al. [69] presented the bending and stress responses of the hybrid axisymmetric system via the state-space method and 3D-elasticity theory. Ma et al. [70] developed the chaotic behavior of graphene-reinforced annular systems under harmonic excitation. Jiao et al. [71] proposed the coupled particle swarm optimization method with a genetic algorithm for the static-dynamic performance of the magneto-electro-elastic nanosystem. Huang et al. [72] have discussed the computer simulation via a couple of homotopy perturbation methods and the generalized differential quadrature method for nonlinear vibration of functionally graded non-uniform micro-tube.

Literature review reveals the lack of an analytical investigation concerning bending of hygro thermo magneto flexo electric nanobeams based on nonlocal elasticity theory. Thus, the authors aimed to construct an analytical model of bending hygro thermo magneto flexo electric nanobeams based on nonlocal elasticity theory.

This paper studied the bending of hygro thermo magneto flexo electric nanobeams (Fig. 1) based on the nonlocal elasticity theory. Governing equations of a nonlocal nanobeam on Winkler-Pasternak substrate are derived via Hamilton's principle. Galerkin method is implemented to solve the governing equations. Effects of different factors such as nonlocal parameter, slenderness, moisture constant, critical temperature, applied voltage and magnet potential, Winkler-Pasternak parameters effect on deflection characteristics of a nanobeam are investigated.

2. Formulation of the Problem

The component of displacement via refined shear deformable beam can be expressed by:

$$u_x(x,z) = u(x) - z\frac{\partial w_b}{\partial x} - f(z)\frac{\partial w_s}{\partial x} \quad (1)$$

$$u_z(x,z) = w_b(x) + w_s(x) u_z(x,z) = w_b(x) + w_s(x) \quad (2)$$

where u is axial mid-plane displacement and w_b, w_s denote the bending and shear components of transverse displacement, respectively. Also, f(z) is the shape function representing the shear stress/strain distribution through the beam thickness, which for the present study has a trigonometric essence; thus, a shear correction factor is not required.

$$f(z) = z + h0 - tan[0.03(z + h0)] \quad (3)$$

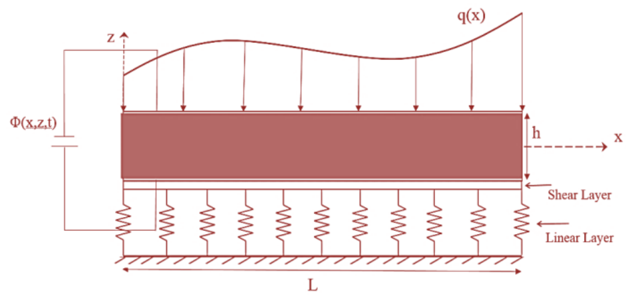

Fig. 1. The geometry of nanobeam resting on elastic foundation

Non-zero strains of the suggested beam model can be expressed as follows:

$$\varepsilon_{xx} = \frac{\partial u}{\partial x} - z\frac{\partial^2 w_b}{\partial x^2} - f(z)\frac{\partial^2 w_s}{\partial x^2} \tag{4}$$

$$\gamma_{xz} = g(z)\frac{\partial w_s}{\partial x} \tag{5}$$

where g(z)=1-df(z)/dz.

According to Maxwell's equation, the relation between electric field (E_x, E_z) and electric potential(ϕ)and magnet field (Q_x, Q_z) and magnet potential (ψ)can be obtained as Ke et al. [41]

$$E_x = -\phi_{,x} = cos(\xi z)\frac{\partial\phi}{\partial x} \qquad Q_x = -\psi_x = cos(\xi z)\frac{\partial\psi}{\partial x} \tag{6}$$

$$E_z = -\phi_{,z} = -\xi\, sin(\xi z)\,\phi - \frac{2v}{h}$$

$$Q_z = -\psi_{,z} = -\xi\, sin(\xi z)\,\psi - \frac{2v}{h} \tag{7}$$

Through extended Hamilton's principle, the governing equations can be derived as follows:

$$\int_0^t \delta(\prod_s - \prod_w)\, dt = 0 \tag{8}$$

where ($\prod_S$) is the total strain energy ($\prod_W$)is the work done by externally applied forces. The first variation of strain energy Π_S can be calculated as:

$$\delta\prod_S = \int_v \sigma_{ij}\delta\varepsilon_{ij}dV = \int_v(\sigma_x\delta\varepsilon_x + \sigma_{xz}\delta\gamma_{xz})dV \tag{9}$$

Substituting Eqs.(1) - (5) into Eq.(9) yields:

$$\delta\prod_S = \int_0^t \begin{pmatrix} N\frac{\partial\delta u}{\partial x} - M_b\frac{\partial^2\delta w_b}{\partial x^2} \\ -M_s\frac{\partial^2\delta w_s}{\partial x^2} + Q\frac{\partial\delta w_s}{\partial x} \end{pmatrix} dx +$$
$$\int_0^a \int_{-\frac{\square}{2}}^{\frac{\square}{2}} \begin{pmatrix} -D_x\, cos(\xi z)\,\delta\left(\frac{\partial\phi}{\partial x}\right) + D_z\xi\, sin(\xi z)\,\delta\phi \\ -B_x\, cos(\xi z)\,\delta\left(\frac{\partial\psi}{\partial x}\right) + B_z\xi\, sin(\xi z)\,\delta\psi \end{pmatrix} dzdx \tag{10}$$

in which the forces and moments expressed in the above equation are defined as follows:

$$[N, M_b, M_s] = \int_A [1, z, f(z)]\sigma_i dA\,, \quad i = (x, y, xy) \tag{11}$$

$$Q = \int_A g(z)\sigma_i dA\,, \quad i(xz, yz)Q = \int_A g(z)\sigma_i dA\,, \quad i(xz, yz)$$

The first variation of the work done by applied forces can be written in the form:

$$\delta\prod_W = \int_0^l \begin{pmatrix} (-N_x^0)\frac{\partial(w_b+w_s)}{\partial x}\frac{\partial\delta(w_b+w_s)}{\partial x} \\ +(N^T + N^H)\frac{\partial(w_b+w_s)}{\partial x}\frac{\partial\delta(w_b+w_s)}{\partial x} \\ -k_w(w_b + w_s)\delta(w_b + w_s) \\ +k_p(w_b + w_s)\frac{\partial^2\delta(w_b+w_s)}{\partial x^2} \\ +f_{13}(w_b + w_s)\delta(w_b + w_s) \end{pmatrix} dx \tag{12}$$

where k_w, andk_p are linear, shear coefficients of the medium, N^E, N^B electric, and magnetic loading, respectively.

$$N_x^0 = N^E + N^B$$

$$N^E = -\int_{-\frac{h}{2}}^{\frac{h}{2}} e_{31}\frac{2V}{h}dz \tag{13}$$

$$N^B = -\int_{-\frac{h}{2}}^{\frac{h}{2}} e_{31}\frac{2\Omega}{h}dz \tag{14}$$

K_w, k_p, and f_{13} are Winkler, Pasternak, and damping constants and N^T, $N^H$are applied forces due to variation of temperature and moisture as

$$N^T = \int_{-h/2}^{h/2} E(z)\alpha_T(z)\Delta T dz \tag{15}$$

$$N^H = \int_{-h/2}^{h/2} E(z)\beta_H(z)\Delta H dz \tag{16}$$

where $\alpha_T(z)$and $\beta_H(z)$ are thermal and moisture expansion coefficients, respectively. T and H denote the temperature and moisture variation, respectively.

The following Euler–Lagrange equations are obtained by inserting Eqs. (10), (12) in Eq. (8) when the coefficients of∂u, ∂w_b, ∂w_s, $\partial\phi$, $\partial\psi$ are equal to zero:

$$\frac{\partial N}{\partial x} = 0 \tag{17}$$

$$\frac{\partial^2 M_b}{\partial x^2} + (-N^E - N^B)\nabla^2(w_b + w_s)$$
$$-(N^T + N^H)\nabla^2(w_b + w_s)$$
$$-k_p\nabla^2(w_b + w_s) + k_w(w_b + w_s) = 0 \tag{18}$$

$$\frac{\partial^2 M_s}{\partial x^2} - \frac{\partial Q}{\partial x} + (-N^E - N^B)\nabla^2(w_b + w_s)$$
$$-(N^T + N^H)\nabla^2(w_b + w_s) - k_p\nabla^2(w_b + w_s)$$

$$+k_w(w_b+w_s)+f_{13}(w_b+w_s)=0 \quad (19)$$

$$\int_{\frac{-h}{2}}^{\frac{h}{2}}\left(\cos(\xi z)\frac{\partial D_x}{\partial x}+D_z\xi\sin(\xi z)\right)dz=0 \quad (20)$$

$$\int_{\frac{-h}{2}}^{\frac{h}{2}}\left(B_x\cos(\xi z)\frac{\partial\delta\psi}{\partial x}+B_z\xi\sin(\xi z)\,\delta\psi\right)dz=0 \quad (21)$$

3. Nonlocal Elasticity Theory

The nonlocal theory can be extended for the piezo magnetic nanobeams as:

$$\sigma_{ij}-(ea)^2\nabla^2\sigma_{ij}=\left[C_{ijkl}\varepsilon_{kl}-e_{mij}E_m-q_{nij}H_n-\alpha_{ij}T-\beta_{ij}H\right] \quad (22)$$

$$D_{ij}-(ea)^2\nabla^2D_{ij}=[e_{ikl}\varepsilon_{kl}+k_{im}E_m+d_{in}H_n] \quad (23)$$

$$B_i-(ea)^2\nabla^2B_i=[q_{ikl}\varepsilon_{kl}+d_{im}E_m+\chi_{in}H_n] \quad (24)$$

$$p_i-(ea)^2\nabla^2p_i=[\varepsilon_0\chi_{ij}E_j+e_{ikl}\varepsilon_{kl}] \quad (25)$$

where c_{ijkl} corresponds with the components of the fourth-order elasticity tensor, also, χ_{ij} is the relative dielectric susceptibility and f_{ijkl} is the flexoelectric coefficient. Also, e_0a is a nonlocal parameter which is introduced to describe the size-dependency of nanostructures.

where ∇^2 is the Laplacian operator. The stress relations can be expressed by:

$$(1-\mu^2\nabla^2)\sigma_{xx}=(1-\lambda^2\nabla^2)[C_{11}\varepsilon_{xx}-e_{31}E_z-q_{31}H_z-\alpha_T\Delta T-\beta_H\Delta H] \quad (26)$$

$$(1-\mu^2\nabla^2)\sigma_{xz}=(1-\lambda^2\nabla^2)[C_{55}\gamma_{xz}-e_{15}E_x-q_{15}H_x] \quad (27)$$

$$(1-\mu^2\nabla^2)D_x=(1-\lambda^2\nabla^2)[e_{15}\gamma_{xz}+k_{11}E_x+d_{11}H_x] \quad (28)$$

$$(1-\mu^2\nabla^2)D_z=(1-\lambda^2\nabla^2)[e_{31}\gamma_{xz}+k_{33}E_z+d_{33}H_z] \quad (29)$$

$$(1-\mu^2\nabla^2)B_x=(1-\lambda^2\nabla^2)[q_{15}\gamma_{xz}+d_{11}E_x+\chi_{11}H_x] \quad (30)$$

$$(1-\mu^2\nabla^2)B_z=(1-\lambda^2\nabla^2)[q_{31}\gamma_{xz}+d_{33}E_z+\chi_{33}H_z] \quad (31)$$

where $\mu=e_0a$ and $\lambda=l$ are nonlocal and length scale parameters.

Integrating Eq. (26-31) over the cross-section area of nanobeam provides the following nonlocal relations for a refined beam model as also, normal forces and moments due to the electrical field can be defined by:

$$M_x=\int_{\frac{-h}{2}}^{\frac{h}{2}}\left(e_{31}\frac{2V}{h}+q_{31}\frac{2\Omega}{h}\right)zdz \quad (32)$$

$$\int_{\frac{-h}{2}}^{\frac{h}{2}}(1-\mu\nabla^2)\{D_x\}\cos(\xi z)dz=F_{11}^e\left\{\frac{\partial\phi}{\partial x}\right\} \quad (33)$$

$$\int_{\frac{-h}{2}}^{\frac{h}{2}}(1-\mu\nabla^2)\{B_x\}\cos(\xi z)dz=R_{11}^e\left\{\frac{\partial\psi}{\partial x}\right\} \quad (34)$$

$$\int_{\frac{-h}{2}}^{\frac{h}{2}}(1-\mu\nabla^2)\{B_x\}\cos(\xi z)dz=R_{11}^e\left\{\frac{\partial\psi}{\partial x}\right\} \quad (35)$$

$$\int_{\frac{-h}{2}}^{\frac{h}{2}}(1-\mu\nabla^2)\{B_x\}\cos(\xi z)dz=R_{11}^e\left\{\frac{\partial\psi}{\partial x}\right\} \quad (36)$$

in which:

$$\{A_{11},B_{11},B_{11}^s,D_{11},D_{11}^s,H_{11}^s\}=\int_{\frac{-h}{2}}^{\frac{h}{2}}C_{11}(1,z,f,z^2,fz,f^2)dz \quad (37)$$

$$(A_{31},E_{31})=\int_{\frac{-h}{2}}^{\frac{h}{2}}e_{31}\xi\sin(\xi z)\{1,z,f\}zdz \quad (38)$$

$$(F_{11},F_{33})=\int_{\frac{-h}{2}}^{\frac{h}{2}}\{s_{11}\cos^2(\xi z),s_{33}\xi^2\sin^2(\xi z)\}dz \quad (39)$$

$$(R_{11},R_{33})=\int_{\frac{-h}{2}}^{\frac{h}{2}}\{d_{11}\cos^2(\xi z),d_{33}\xi^2\sin^2(\xi z)\}dz \quad (40)$$

$$(G_{31},Q_{31})=\int_{\frac{-h}{2}}^{\frac{h}{2}}q_{31}\xi\sin(\xi z)\{1,z\}zdz \quad (41)$$

$$(\chi_{11},\chi_{33})=\int_{\frac{-h}{2}}^{\frac{h}{2}}\{\chi_{11}\cos^2(\xi z),\chi_{33}\xi^2\sin^2(\xi z)\}dz \quad (42)$$

The governing equations of nonlocal strain gradient nanoplate under electrical field in terms of the displacement can be derived by substituting Eqs. (32) - (۳6), into Eqs. (17) - (21) as follows:

$$\left[A_{11}\frac{\partial^2u}{\partial x^2}-B_{11}\frac{\partial^3w_b}{\partial x^3}-B_{11}^s\frac{\partial^3w_s}{\partial x^3}+A_{31}\frac{\partial\phi}{\partial x}+G_{31}\frac{\partial\psi}{\partial x}\right]=\frac{\partial N_x}{\partial x} \quad (43)$$

$$\begin{bmatrix}B_{11}\dfrac{\partial^3u}{\partial x^3}-D_{11}\dfrac{\partial^4w_b}{\partial x^4}-D_s^{11}\dfrac{\partial^4w_s}{\partial x^4}+E_{31}\dfrac{\partial^2\phi}{\partial x^2}\\+Q_{31}\dfrac{\partial^2\psi}{\partial x^2}+k_p\nabla^2(w_b+w_s)-k_w(w_b+w_s)\end{bmatrix}-\mu\begin{bmatrix}(-N^E-N^B)+(N^T+N^H)\nabla^2(w_b+w_s)\\+k_p\nabla^2(w_b+w_s)-k_w(w_b+w_s)\end{bmatrix}=\frac{\partial^2M_b}{\partial x^2} \quad (44)$$

$$\begin{bmatrix}B_{11}^s\dfrac{\partial^3u}{\partial x^3}-D_{11}^s\dfrac{\partial^4w_b}{\partial x^4}-D_{11}^s\dfrac{\partial^4w_s}{\partial x^4}+F_{11}\dfrac{\partial^2\phi}{\partial x^2}+R_{11}\dfrac{\partial^2\psi}{\partial x^2}\\+k_p\nabla^2(w_b+w_s)+f_{13}\delta(w_b+w_s)-k_w(w_b+w_s)\end{bmatrix}$$

$$-\mu\begin{bmatrix}(-N^E-N^B)+(N^T+N^H)\nabla^2(w_b+w_s)\\+k_p\nabla^2(w_b+w_s)-k_w(w_b+w_s)\end{bmatrix}=\frac{\partial^2 M_b}{\partial x^2}-\frac{\partial Q}{\partial x} \quad (45)$$

$$A_{31}\frac{\partial u}{\partial x}-E_{31}\frac{\partial^2 w_b}{\partial x^2}-Q_{31}\frac{\partial^2 w_s}{\partial x^2}+F_{11}\frac{\partial^2\phi}{\partial x^2}+R_{11}\frac{\partial^2\psi}{\partial x^2}-F_{33}\phi-F_{33}\psi=0 \quad (46)$$

$$A_{31}\frac{\partial u}{\partial x}-E_{31}\frac{\partial^2 w_b}{\partial x^2}-Q_{31}\frac{\partial^2 w_s}{\partial x^2}+\chi_{11}\frac{\partial^2\phi}{\partial x^2}+R_{11}\frac{\partial^2\psi}{\partial x^2}-F_{33}\phi-\chi_{33}\psi=0 \quad (47)$$

4. Solution Procedure

The displacement quantities are presented in the following form to satisfy the boundary conditions (given in Table 1) as :

$$u=\sum_{n=1}^{\infty}U_n\frac{\partial X_n(x)}{\partial x}e^{i\omega_n t} \quad (48)$$

$$w_b=\sum_{n=1}^{\infty}W_{bn}X_n(x)\,e^{i\omega_n t} \quad (49)$$

$$w_s=\sum_{n=1}^{\infty}W_{sn}X_n(x)\,e^{i\omega_n t} \quad (50)$$

$$\phi=\sum_{n=1}^{\infty}\phi_n X_n(x)\,e^{i\omega_n t} \quad (51)$$

$$\psi=\sum_{n=1}^{\infty}\psi_n X_n(x)\,e^{i\omega_n t} \quad (52)$$

where (U_n ,W_{bn}, W_{sn},ϕ_n, ψ_n) are the unknown coefficients and for different boundary conditions ($\alpha=m\pi/a,\beta=n\pi/b$) :

$$[K]\begin{Bmatrix}u_n\\w_{bn}\\w_{sn}\\\phi\\\psi\end{Bmatrix}=\begin{Bmatrix}0\\Q_n(1+\mu\frac{n^2\pi^2}{L^2})\\Q_n(1+\mu\frac{n^2\pi^2}{L^2})\\0\\0\end{Bmatrix} \quad (53)$$

where [K], and [F] are the stiffness, loading matrixes for nanobeam, respectively.

$$k_{1,1}=A_{11}\alpha_1,\quad k_{1,2}=B_{11}\alpha_2,\quad k_{1,3}=B^s_{11}\alpha_2,$$
$$k_{1,4}=A_{31}\alpha_3,\quad k_{1,5}=G_{31}\alpha_3 \quad (54)$$
$$k_{2,1}=B_{11}\alpha_{11},$$
$$k_{2,2}=-D_{11}\alpha_7+k_w\alpha_5-k_p\alpha_6+\mu\left[((-N^E-N^B)+(N^T+N^H)+k_p)\alpha_6-k_w\alpha_5\right],$$
$$k_{2,3}=-D^s_{11}\alpha_7+k_w\alpha_5-k_p\alpha_6+\mu\left[((-N^E-N^B)+(N^T+N^H)+k_p)\alpha_6-k_w\alpha_5\right]$$
$$k_{2,4}=E_{31}\alpha_6,\quad k_{2,5}=Q_{31}\alpha_6,$$
$$k_{3,1}=B^s_{11}\alpha_{11},$$
$$k_{3,2}=-D^s_{11}\alpha_7+\mu\left[((-N^E-N^B)+(N^T+N^H)+k_p)\alpha_6-k_w\alpha_5\right],$$
$$k_{3,3}=-H^s_{11}\alpha_7+k_w\alpha_5-k_p\alpha_6+\mu\begin{bmatrix}((-N^E-N^B)+(N^T+N^H)+k_p)\alpha_6\\-(k_w+\frac{e_{31}}{2k_{33}})f_{13}\alpha_5\end{bmatrix}$$
$$k_{3,4}=F_{11}\alpha_6,\quad k_{2,5}=R_{11}\alpha_6,$$
$$k_{4,1}=A_{31}\alpha_3,\quad k_{4,2}=-E_{31}\alpha_6,\quad k_{4,3}=-Q_{31}\alpha_6,$$
$$k_{4,4}=F_{11}\alpha_6-F_{33}\alpha_5,\quad k_{4,5}=R_{11}\alpha_6-R_{33}\alpha_5$$
$$k_{5,1}=A_{31}\alpha_3,\quad k_{5,2}=-E_{31}\alpha_6,\quad k_{5,3}=-Q_{31}\alpha_6,$$
$$k_{5,4}=F_{11}\alpha_6-F_{33}\alpha_5,\quad k_{5,5}=\chi_{11}\alpha_6-\chi_{33}\alpha_5$$
$$F_{1,1}=N\alpha_3,$$
$$F_{2,2}=M_b(1-\mu\alpha_6),$$
$$F_{3,3}=M_s(1-\mu\alpha_6)-Q(1-\mu\alpha_3),$$

in which:

$$\alpha_1=\int_0^a X'(x)X''(x)dx,\quad \alpha_2=\int_0^a X(x)X'''(x)dx,$$
$$\alpha_7=\int_0^a X(x)X''''(x)dx\quad \alpha_5=\int_0^a X(x)X(x)dx,$$
$$\alpha_3=\int_0^a X(x)X'(x)dx,\quad \alpha_{11}=\int_0^a X'(x)X''''(x)dx,$$
$$\alpha_6=\int_0^a X(x)X''(x)dx \quad (55)$$

Table 1. The admissible functions $X_m(x)$ Sobhy [38]

	Boundary conditions	The functions X_n
	At x=0, a	$X_n(x)$
SS	$X_n=0, X''_n=0$	$sin(\alpha x)$
	$X_n(a)=0, X''_n(a)=0$	

The uniform load is supposed that lead to bending and is expressed by the following form:

$$q_{dynamics}=\sum_{n=1}^{\infty}Q_n\,sin[\frac{n\pi}{L}x]\,sin\,\omega\,t \quad (56)$$

$$Q_n = \frac{2}{L}\int_{x_0\text{-}c}^{x_0+c} \sin[\frac{n\pi}{L}x] q_x dx \quad (57)$$

Qn is the Fourier coefficient, q(x) = q_0 is the uniform load density, and x_0 is the centroid coordinate. Also, in the case of concentrated point load, the following expression for the harmonic load intensity can be written:

$$q(x) = p\delta(x\text{-}x_0) \sin \omega t \quad (58)$$

$$Q_n = \frac{2p}{L} \sin[\frac{n\pi}{L} x_0] \quad (59)$$

in which δ is the Dirac delta.

5. Numerical Results and Discussions

The bending of hygro magneto thermos piezoelectric nanobeam is analyzed in this section. The material properties are shown in Table 2 (Ramirez et al. [42]). The validity of the present study is proved by comparing the bending of this model with those of Arefi and Zenkour [31]. Arefi and Zenkour [31] for various nonlocal parameters as presented in Table 3. The role of multiple parameters like magnetic potential (Ω), electric voltage (V), moisture constant (ΔH), and nonlocal parameter (μ) on the non-dimensional frequencies of the supported higher-order magneto-electro-elastic nanobeams at L/h=20 and L/h=30 are exposed in Tables 4 and Table 5. Here, it is noticeable that with the rise of nonlocal parameters, the natural frequencies of hygro magneto-electro-elastic nanobeam reduce for all magnetic potentials and external voltages due to the existence of nonlocality weakens the beam. Also, it is referred that when the moisture constant arose, the non-dimensional frequencies of hygro magneto-electro-elastic nanobeam decreased, especially for lower moisture constant. Moreover, it is concluded that negative values of magnetic potential and external electric voltage produce lower/higher frequencies than positive ones.

The length of the nanobeam is considered to be L = 10 nm.

Also, the dimensionless deflection is adopted as

$$W = 100\frac{C_{11}I}{q_0 L^4} \quad (60)$$

Figures 2 and 3 are investigated for the effect of nonlocal parameters on a dimensionless deflection through various magnetic potentials. The increasing value of nonlocal parameter caused an increase of dimensionless deflection, but positive electric voltage leads to a reduction in deflection and negative potential rise the dimensionless deflection. We understand from this subject that magnetic potential has a significant role under dimensionless deflection and dimensionless deflection null effect during zero electric voltage. It must be mentioned that the nonlocal parameter weakens the nanobeam structure. The impact of humid is observed in Fig.3 through the rise in dimensionless deflection.

Dimensionless deflection of the nanobeam concerning slenderness ratio through various electric voltages are presented in Figs. 4 and 5. It is found that the external electric voltage caused that softening deflection of nanobeam for positive values and external voltage for negative values of nanobeam demonstrated a hardening effect. From this, the axial tensile and compressive forces are exposed in the nanobeams via the constructed positive and negative voltages, respectively. In addition, it is lightly observed that the dimensionless deflection is approximately independent of the slenderness ratio for zero electric voltages ($V = 0$). The increase in magnetic potential hardens the deflection.

Table 2. Material properties of BiTiO3-CoFe2O4 composite material

Properties	BiTiO3-CoFe2O4
Elastic (GPa)	
$c11$ = 226, $c12$ = 125, $c13$ = 124, $c33$ = 216, $c44$ = 44.2, $c66$ = 50.5	
Piezoelectric/(C・m^{-2})	$e31 = -2.2$, $e33 = 9.3$, $e15 = 5.8$
Dielectric/(10^{-9}C・V^{-1}・m^{-1})	$k11 = 5.64$, $k33 = 6.35$
Piezomagnetic/(N・A^{-1}・m−1)	
$q15 = 275$, $q31 = 290.1$, $q33 = 349.9$	
Magnetoelectric/(10^{-12}Ns・V^{-1}・C^{-1})	
$s11 = 5.367$, $s33 = 2\,737.5$	
Magnetic (10^{-6} $Ns^2\,c^{-2}/2$)	$-\varkappa_{11} = 297, \varkappa_{33} = 83.5$
Mass density (Kg/m3)	ρ=5.55
Hygrothermal(/K)	$\alpha_{eff} = 1.6\times10^{-6}$ $\beta_{eff} = 26\times10^{-4}$

Table 3. Comparison of dimensionless deflections of nanobeam for electric voltage and magnetic potential.

L/h	μ (nm²)	$\psi = 0.001$		L/h	μ (nm²)	$\phi = 0.001$	
		Arefi and Zenkour (2016)	Present			Arefi and Zenkour (2016)	Present
10	1	3.68	3.5781	10	0	3.68	3.59892
	2	3.71	3.6482		1	1.3333	.66921
	3	3.77	3.7302		2	1.3645	3.74018
	4	3.84	3.79011		3	1.3958	3.80234
	5	3.94	3.8952		4	1.4270	3.92011

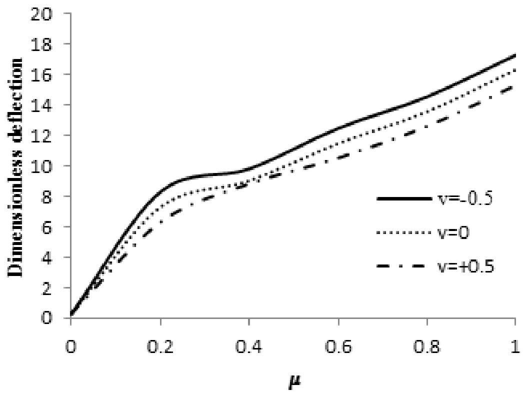

Fig. 2. Effect of nonlocal parameters on dimensionless deflection via $\Omega = 0.5$ (L/h=10,,K_w= K_p=20,ΔH=1.5).

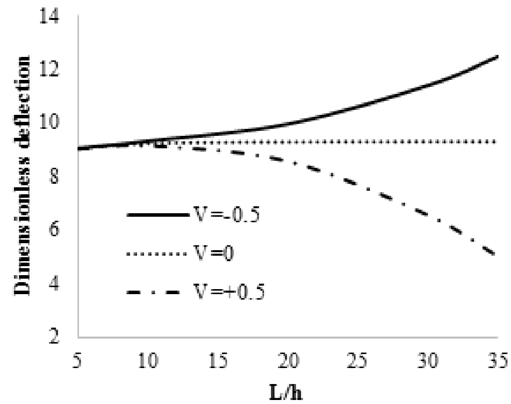

Fig. 4. Effect of slenderness ratio on dimensionless deflection via $\Omega = 0.5$ (L/h=10,,K_w= K_p=20,ΔH=1.5).

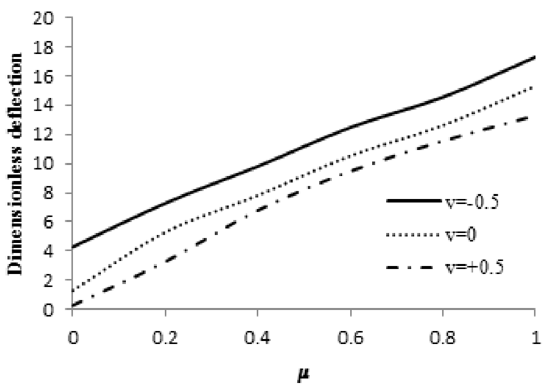

Fig. 3. Effect of nonlocal parameters on dimensionless deflection via $\Omega = 1.5$ (L/h=10,,K_w= K_p=20,ΔH=1.5).

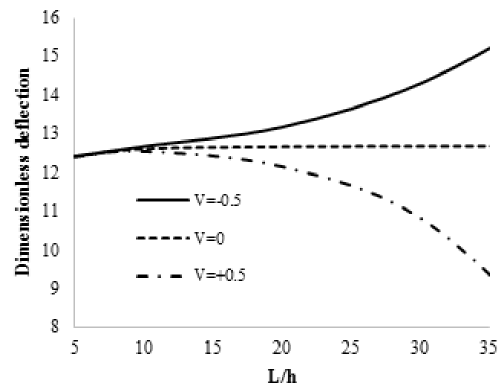

Fig. 5. Effect of slenderness ratio on dimensionless deflection via $\Omega = 1.5$ (L/h=10,,K_w= K_p=20,ΔH=1.5).

Table 4. Variation of dimensionless frequency of FG nanobeam for the various nonlocal parameter, magnetic potentials, and electric voltages (L/h =20).

μ		Ω=-0.05			Ω=0			Ω=+0.05		
		ΔH =0.2	ΔH =1	ΔH =5	ΔH =0.2	ΔH =1	ΔH =5	ΔH =0.2	ΔH =1	ΔH =5
0	V=-5	35.6083	32.9563	31.4249	36.477	33.5046	31.6119	37.3256	34.044	31.7979
	V=0	35.4747	32.5345	30.7053	36.3466	33.0897	30.8967	37.1982	33.6358	31.0870
	V=+5	35.3406	32.1071	29.9685	36.2158	32.6696	30.1646	37.0703	33.2226	30.3594
1	V=-5	29.9003	27.8605	26.7829	30.9298	28.5069	27.0022	31.9261	29.1390	27.2197
	V=0	29.7411	27.3602	25.9349	30.7759	28.0182	26.1613	31.7771	28.6610	26.3857
	V=+5	29.5810	26.8506	25.0582	30.6212	27.5207	25.2924	31.6273	28.1749	25.5245
2	V=-5	26.1741	24.5567	23.7980	27.3442	25.2877	24.0444	28.4663	25.9981	24.2884
	V=0	25.9920	23.9876	22.8394	27.1700	24.7354	23.0961	28.2990	25.4613	23.3500
	V=+5	25.8087	23.4046	21.8388	26.9947	24.1705	22.1071	28.1307	24.9128	22.3722
3	V=-5	23.4875	22.1912	21.6780	24.7848	22.9976	21.9483	26.0176	23.7765	22.2153
	V=0	23.2845	21.5598	20.6211	24.5925	22.3889	20.9050	25.8344	23.1883	21.1852
	V=+5	23.0796	20.9093	19.5070	24.3987	21.7631	19.8069	25.6500	22.5847	20.1024

Table 5. Dispersion of dimensionless frequency of nanobeam for the various nonlocal parameter, magnetic potentials, and electric voltages (L/h =30).

μ		Ω=-0.05			Ω=0			Ω=+0.05		
		ΔH =0.2	ΔH =1	ΔH =5	ΔH =0.2	ΔH =1	ΔH =5	ΔH =0.2	ΔH =1	ΔH =5
0	V=-5	35.5080	32.1523	30.4349	36.376	33.11246	31.534	37.2222	33.144	30.7779
	V=0	34.4347	32.345	30.234	36.1466	32.0997	30.5967	36.0982	33.445	30.8870
	V=+5	35.3406	32.0061	29.0685	36.0158	32.6096	30.0646	36.0703	33.0226	29.3294
1	V=-5	29.789	27.456	26.657	30.567	28.2349	26.4022	31.0261	29.0290	27.123
	V=0	29.5411	27.3002	25.7249	30.6559	27.8182	26.0613	31.6771	28.5610	26.4857
	V=+5	29.423	26.6506	24.7582	30.3212	27.0007	25.134	31.5273	28.0549	25.235
2	V=-5	26.0241	24.327	23.5680	27.1242	25.0877	23.8444	28.0663	25.7781	24.145
	V=0	25.754	23.4876	22.344	27.0500	24.524	22.5961	28.0990	25.0613	23.0500
	V=+5	25.567	23.3046	21.728	26.337	24.0705	22.0071	28.0307	24.7128	22.0722
3	V=-5	23.0875	22.0912	21.210	24.6248	22.3476	21.6483	25.0176	23.5765	22.1153
	V=0	23.0845	21.2398	20.5211	24.4325	22.2889	20.6050	25.6344	23.0883	21.0852
	V=+5	22.0796	20.723	19.3070	24.2787	21.7001	19.4069	25.5500	22.4847	20.0024

In Figs. 6 and 7, the demonstration for the variation of dimensionless deflection of nanobeam with the moisture constant with different electric voltage via various magnetic potentials is given. From this, it is obtained that the rise in moisture constants weakens the value of deflection. Also, it is referred that the positive voltage values increase the stiffness than negative voltage. The obtained results of these figures indicate that the maximum deflection increases with increasing the magnetic potential of the nanobeam. Figures 8 and 9 expose the effect of critical temperature on the dimensionless deflection via moisture coefficient rise with different electric voltage values. It can be noticed that the increase in critical temperature drives to reduce the dimensionless deflection. Also, the moisture coefficient rise exposes the less magnitude rise in dimensionless deflection while increasing temperature values. The results reveal the truth that the moisture coefficient variations soften the variant values via critical temperature.

The variations of the dimensionless deflection of nanobeams versus the Winkler and Pasternak parameters for various electric voltages are shown in Fig.10 and 11, respectively. It is found from this figure that regardless of the sign and magnitude of electric voltage, the dimensionless deflection increases with the increase of Winkler and Pasternak parameters, So the increment in stiffens of the nanobeam. At a constant electric voltage, the growth of dimensionless defection with Pasternak parameter measurement has a higher rate than the Winkler parameter.

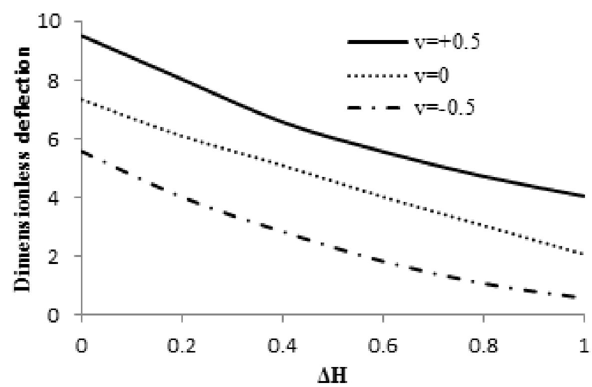

Fig. 6. Effect of moisture constant versus dimensionless deflection via , Ω = 0.5 (L/h=10, K_p =K_w=20).

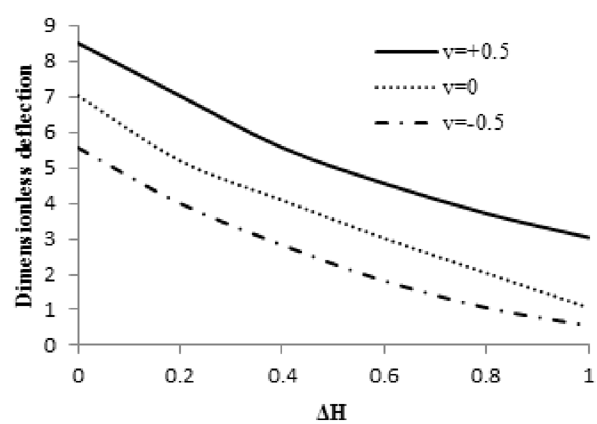

Fig. 7. Effect of moisture constant versus dimensionless deflection via Ω = 1.5 (L/h=10, K_p =K_w=20).

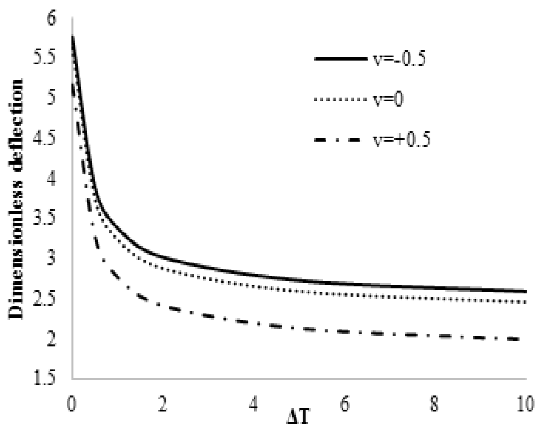

Fig. 8. Effect of critical temperature versus dimensionless deflection via ΔH=0.5 (L/h=10, K_p =K_w=20, $\Omega = 0$).

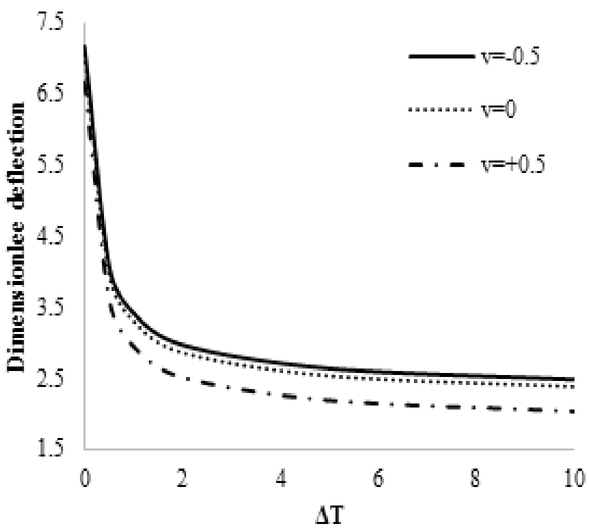

Fig. 9. Effect of critical temperature versus dimensionless deflection via ΔH=1.5 (L/h=10, K_p =K_w=20, $\Omega = 0$).

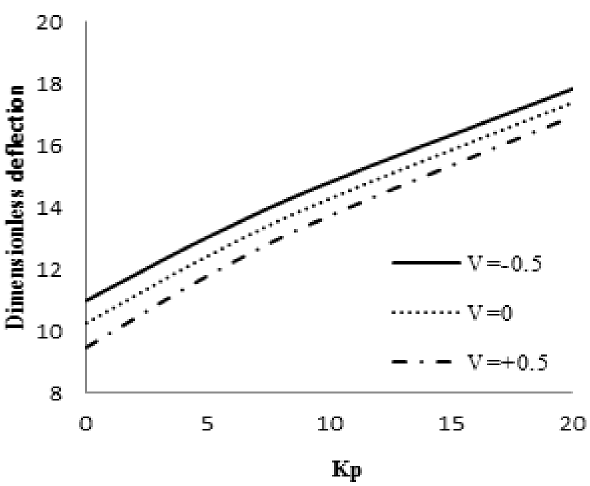

Fig. 10. Effect of the Pasternak foundation versus dimensionless deflection (L/h=10, $\Omega = 0$,$\mu = 2, \Delta H = 1.5$).

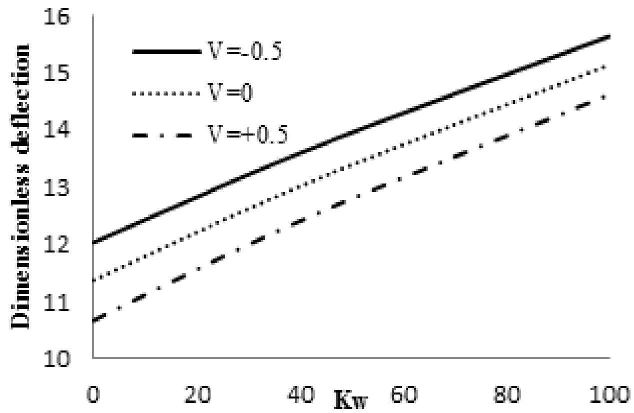

Fig. 11. Effect of the Winkler foundation versus dimensionless deflection (L/h=10, $\Omega = 0$,$\mu = 2, \Delta H = 1.5$).

6. Conclusion

External electric voltages on the deflection of Hygro-magneto-electro-elastic (HMEE) embedded nanobeams are studied in this article. The governing equations of nonlocal nanobeams based on higher-order refined beam theory are obtained using Hamilton's principle and solved by an analytical solution. A parametric study is presented to observe the effect of the nonlocal parameter, slenderness, moisture constant, critical temperature, and the foundation constants on the deflection characteristics of nanobeam via different applied electric voltages. Some of the bolded highlights of this research are as follows.

1. The dimensionless deflection can be amplified using a higher nonlocal parameter.
2. The maximum dynamic response can be arrived at by choosing higher magnetic intensity.
3. The system's dimensionless deflection can be gradually amplified when the electric voltage is negative.
4. The moisture values soften the dimensionless deflection in the presence of magnetic potential.
5. The dimensionless deflection may be weakened by bigger values of critical temperature in a humid environment.
6. The Pasternak parameters propose a higher deflection than the Winkler parameter when the applied electric voltage is constant.
7. The compressive and tensile nature is proven to deflect nanobeams via positive and negative voltage generation.

References

[1] Van Den Boomgard, J., Terrell, D.R. and Born, R.A.J., 1974. An in situ grown eutectic magnetoelectric

composite material. *Journal of Materials Science*, *9*, pp.1705–1709.
[2] Zheng, H., Wang J. and Lofland S.E., 2004. Multiferroic BaTiO3-CoFe2O4 nanostructures. *Science*, *303*, pp.661–663.
[3] Martin, L.W., Crane, S.P. and Chu, Y.H., 2008. Multiferroics and magnetoelectrics: Thin films and nanostructures. *Journal of Condensed Matter Physics*, *20*, pp.434220.
[4] Wang, Y., Hu, J.M. and Lin, Y.H., 2010. Multiferroic magnetoelectric composite nanostructures. *NPG Asia Mater*, *2*, pp.61–68.
[5] Prashanthi, K., Shaibani, P.M. and Sohrabi A., 2012. Nanoscale magnetoelectric coupling in multiferroic BiFeO3 nanowires. *Physica Status Solidi-Rapid Research*, *6*, pp.244–246.
[6] Eringen, A., 1968. Mechanics of micromorphic continua, in E. Kroner (Ed.), Mechanics of Generalized Continua. *Springer-Verlag*, *104*, pp.18–35.
[7] Eringen, A., 1972. Nonlocal polar elastic continua. *International Journal of Engineering Science*, *10*, pp.1–16.
[8] Eringen, A., 1976. Nonlocal micropolar field theory, In Continuum Physics. *Eringen A.C. (Ed.) Academic Press, New York*, *106*.
[9] Eringen, A., 2002. Nonlocal Continuum Field Theories. *Springer, New York*, *105*.
[10] Yang, J., Ke, L.L. and Kitipornchai, S., 2010. Nonlinear free vibration of single-walled carbon nanotubes using nonlocal Timoshenko beam theory. *Physica E: Low-dimensional Systems and Nanostructures*, *42*, pp.1727-1735.
[11] Ehyaei, J. and Akbarizadeh, M.R., 2017. Vibration-analysis of micro composite thin beam based on modified couple stress. *Structural Engineering and Mechanics*, *64*, pp.793-802.
[12] Ebrahimi, F. and Barati, M.R., 2016. Buckling analysis of nonlocal third-order shear deformable functionally graded piezoelectric nanobeams embedded in elastic medium. *Journal of the Brazilian Society of Mechanical Sciences and Engineering*, *39*, pp.937-952.
[13] Dihaj, A., Zidour, M., Meradjah, M., Rakrak, K., Heireche, H. and Chemi, A., 2018. Free vibration analysis of chiral double-walled carbon nanotube embedded in an elastic medium using non-local elasticity theory and Euler Bernoulli beam model. *Structural Engineering and Mechanics*, *65*(3), pp.335-342.
[14] Ebrahimi, F. and Barati, M.R., 2016a. Dynamic modeling of a thermo–piezo-electrically actuated nanosize beam subjected to a magnetic field. *Applied Physics*, *122*(4), pp.1-18.
[15] Ebrahimi, F. and Barati, M.R., 2016b. Electromechanical buckling behavior of smart piezoelectrically actuated higher-order size-dependent graded nanoscale beams in thermal environment. *International Journal of Smart and Nano Materials*, *7*(2), pp.69-70.
[16] Ebrahimi, F. and Barati, M.R., 2016c. An exact solution for buckling analysis of embedded piezoelectro-magnetically actuated nanoscale beams. *Advance Nano Research*, *4*, pp.65-84.
[17] Ebrahimi, F. and Barati, M.R., 2016d. Vibration analysis of smart piezoelectrically actuated nanobeams subjected to magneto-electrical field in thermal environment. *Journal of Vibration and Control*, 1077546316646239.
[18] Roque, C.M.C., Ferreira, A.J.M. and Reddy, J.N., 2011. Analysis of Timoshenko nanobeams with a nonlocal formulation and meshless method. *International Journal of Engineering Science*, *49*, pp.976-984.
[19] Peddieson, J., Buchanan, G.R. and Mcnitt, R.P., 2003. Application of nonlocal continuum models to nanotechnology. *International Journal of Engineering Science*, *41*, pp.305–312.
[20] Civalek, O. and Demir, C., 2011. Bending analysis of microtubules using nonlocal Euler–Bernoulli beam theory. *Applied Mathematical Sciences*, *35*, pp.2053–2067.
[21] Wang Q., 2005. Wave propagation in carbon nanotubes via nonlocal continuum mechanics. *Journal of Applied Physics*, *98*, pp.124-301.
[22] Wang, C.M., Kitipornchai, S., Lim, C.W. and Eisenberger, M., 2008. Beam bending solutions based on nonlocal Timoshenko beam theory. *Journal of Engineering Mechanics*, *134*, pp.475–481.
[23] Murmu, T. and Pradhan, S.C., 2009. Buckling analysis of a single-walled carbon nanotube embedded in an elastic medium based on nonlocal elasticity and Timoshenko beam theory and using DQM. *Physica E: Low-dimensional Systems and Nanostructures*, *41*, pp.1232-1239.
[24] Karami, B., Janghorban, M. and Tounsi, A., 2017. Effects of triaxial magnetic field on the anisotropic nanoplates. *Steel and Composite Structure*, *25*, pp.361-374.
[25] Ebrahimi, F. and Rostami, P., 2018. Propagation of elastic waves in thermally affected embedded carbon-nanotube-reinforced composite beams via various shear deformation plate theories. *Structural Engineering and Mechanics*, *66*, pp.495-504.

[26] Hajnayeb, A.K.A. and Foruzande, H. 2017. Free vibration analysis of a piezoelectric nanobeam using nonlocal elasticity theory. *Structural Engineering and Mechanics*, *61*, pp.617-624.
[27] Ebrahimi, F., jafari, A. and Selvamani, R., 2020. Thermal buckling analysis of magneto electro elastic porous FG beam in thermal environment. *Advances in Nano Research*, *8*, pp.83-94.
[28] Ebrahimi, F., Hamed, S., Hosseini, S. and Selvamani, R., 2020. Thermo-electro-elastic nonlinear stability analysis of viscoelastic double-piezo nano plates under magnetic field. *Structural engineering and mechanics*, *73*, pp.565-584,
[29] Ebrahimi, F., Kokaba, M., Shaghaghi, G. and Selvamani, R., 2020. Dynamic characteristics of hygro-magneto-thermo-electrical nanobeam with non- ideal boundary conditions. *Advances in Nano Research*, *8*, pp.169-182.
[30] Yazdi, A.A., 2018. Large amplitude forced vibration of functionally graded nano-composite plate with piezoelectric layers resting on nonlinear elastic foundation. *Structural Engineering and Mechanics*, *68*, pp.203–213.
[31] Arefi, M. and Zenkour, A.M., 2016. A simplified shear and normal deformations nonlocal theory for bending of functionally graded piezomagnetic sandwich nanobeams in magneto-thermo-electric environment. *Journal of Sandwich Structures and Materials*, *18*, pp.624-651.
[32] Ebrahimi, F. and Barati, M.R., 2018. Wave propagation analysis of smart strain gradient piezo-magneto-elastic nonlocal beams. *Structural Engineering and Mechanics*, *66*, pp.237-248.
[33] Arefi, M., 2019. Static analysis of laminated piezo-magnetic size-dependent curved beam based on modified couple stress theory. *Structural Engineering and Mechanics*, *69*, pp.145-153.
[34] Aimin, J. and Haojiang, D., 2004. Analytical solutions to magneto-electro-elastic beams. *Structural Engineering and Mechanics*, *18*, pp.195-209.
[35] Gayen, D. and Roy, T., 2013. Hygro-thermal effects on stress analysis of tapered laminated composite beam. *International Journal of Composite Materials*, *3*, pp.46–55.
[36] Kurtinaitiene, M., Mazeika, K., Ramanavicius, S., Pakstas, V. and Jagminas, A., 2016. Effect of additives on the hydrothermal synthesis of manganese ferrite nanoparticles. *Advances in Nano Research*, *4*, pp.1-14.
[37] Alzahrani, E.O., Zenkour, A.M. and Sobhy, M., 2013. Small scale effect on hygro-thermo-mechanical bending of nanoplates embedded in an elastic medium. *Composite Structures*, *105*, pp.163-172.
[38] Sobhy, M., 2013. Buckling and free vibration of exponentially graded sandwich plates resting on elastic foundations under various boundary conditions. *Composite structure*, *99*, pp.76-87.
[39] Ghorbanpour Arani, A. and Zamani, M.H., 2017. Investigation of electric field effect on size-dependent bending analysis of functionally graded porous shear and normal deformable sandwich nanoplate on silica Aerogel foundation. *Journal of Sandwich Structures and Materials*, *21*, 109963621772140.
[40] Şimşek, M. and Yurtcu, H.H., 2013. Analytical solutions for bending and buckling of functionally graded nanobeams based on the nonlocal Timoshenko beam theory. *Composite Structures*, *97*, pp.378-386.
[41] Ke, L.L, Wang, Y.S., Yang, J. and Kitipornchai, S., 2014. Free vibration of size-dependent magneto-electro-elastic nano plates based on the nonlocal theory. *Acta Mechanica Sinica*, *30*, pp.516-525.
[42] Ramirez, F., Heyliger, P.R. and Pan, E., 2006, Discrete layer solution to free vibrations of functionally graded magneto-electro-elastic plates, *Mechanics of Advanced Materials and Structure*, *13*, pp.249-266.
[43] Zur, K.K., Arefi, M., Kim, J. and Reddy, J.N., 2020. Free vibration and buckling analyses of magneto-electro-elastic FGM nanoplates based on nonlocal modified higher-order sinusoidal shear deformation theory. *Composites Part B: Engineering 182*, pp.107601.
[44] Arefi, M., Kiani, M. and Rabczuk, T., 2019. Application of nonlocal strain gradient theory to size dependent bending analysis of a sandwich porous nanoplate integrated with piezomagnetic face-sheets. *Composites Part B: Engineering*, *168*, pp.320-333.
[45] Arefi, M. and Zenkour, A.M., 2017. Thermo-electro-mechanical bending behavior of sandwich nanoplate integrated with piezoelectric face-sheets based on trigonometric plate theory. *Composite Structures*, *162*, pp.108-122.
[46] Arefi, M. and Zenkour, A.M., 2017. Nonlocal electro-thermo-mechanical analysis of a sandwich nanoplate containing a Kelvin–Voigt viscoelastic nanoplate and two piezoelectric layers. *Acta Mechanica*, *228*, pp.475–493.
[47] Arefi, M., Mohammad-Rezaei Bidgoli, E., Dimitri, R. and Tornabene, F., 2018, Free vibrations of functionally graded polymer composite nanoplates reinforced with graphene nanoplatelets. *Aerospace Science and Technology*, *81*, pp.108-117.

[48] Arefi, M. and Zenkour, A.M., 2018. Size-dependent electro-elastic analysis of a sandwich microbeam based on higher-order sinusoidal shear deformation theory and strain gradient theory. *Journal of Intelligent Material Systems and Structures*, *29*(7), pp.1394-1406.

[49] Arefi, M. and Rabczuk, T., 2019. A nonlocal higher order shear deformation theory for electro-elastic analysis of a piezoelectric doubly curved nano shell. *Composites Part B: Engineering*, *168*, pp.496-510.

[50] Barati, M.R., Faleh, N. and Zenkour, A.M., 2019. Dynamic response of nanobeams subjected to moving nanoparticles and hygro-thermal environments based on nonlocal strain gradient theory. *Mechanics of Advanced Materials and Structures*, *26*(19), pp.1661-1669.

[51] Arefi, M. and Zenkour, A.M., 2019. Influence of magneto-electric environments on size-dependent bending results of three-layer piezomagnetic curved nanobeam based on sinusoidal shear deformation theory. *Journal of Sandwich Structures and Materials*, *21*(8), pp.2751–2778.

[52] Arefi, M. and Zenkour, A.M., 2018. Size-dependent vibration and electro-magneto-elastic bending responses of sandwich piezomagnetic curved nanobeams. *Steel and Composite Structures*, *29*(5), pp.579–590.

[53] Zenkour, A.M. and Alghanmi, R., 2020. Static response of sandwich plates with FG core and piezoelectric faces under thermo-electro-mechanical loads and resting on elastic foundations. *Thin-Walled Structures*, *157*, pp.107025.

[54] Sobhy, M. and Zenkour, A., 2020. The modified couple stress model for bending of normal deformable viscoelastic nanobeams resting on visco-Pasternak foundations. *Mechanics of Advanced Materials and Structures*, *27*(7), pp.525–538.

[55] Zenkour, A.M. and El-Shahrany, H.D., 2020. Vibration suppression of magnetostrictive laminated beams resting on viscoelastic foundation. *Applied Mathematics and Mechanics*, *41*(8), pp.1269–1286.

[56] Barati, M.R. and Zenkour, A.M., 2018. Forced vibration of sinusoidal FG nanobeams resting on hybrid Kerr foundation in hygro-thermal environments. *Mechanics of Advanced Materials and Structures*, *25*(8), pp.669–680.

[57] Daik, A. and Zenkour, A.M., 2020. Bending of Functionally Graded Sandwich Nanoplates Resting on Pasternak Foundation under Different Boundary Conditions. *Journal of Applied and Computational Mechanics*, *6*, pp.1245–1259.

[58] Guo, Y., Mi, H. and Habibi, M., 2021. Electromechanical energy absorption, resonance frequency, and low-velocity impact analysis of the piezoelectric doubly curved system. *Mechanical Systems and Signal Processing*, *157*, pp.107723.

[59] Dai, Z., Zhang Z., Yasaman Bolandi, S. and Habibi, M., 2021. On the vibrations of the non-polynomial viscoelastic composite open-type shell under residual stresses. *Composite Structures*, *263*, pp.113599.

[60] Wu, J. and Habibi, M., 2021. Dynamic simulation of the ultra-fast-rotating sandwich cantilever disk via finite element and semi-numerical methods. *Engineering with Computers*. https://doi.org/10.1007/s00366-021-01396-6

[61] Al-Furjan, M.S.H., Samimi-Sohrforozani, E., Habibi, M., Jung, D.W. and Safarpour, H., 2021. Vibrational characteristics of a higher-order laminated composite viscoelastic annular microplate via modified couple stress theory. *Composite Structures*, *257*, pp.113152.

[62] Al-Furjan, M.S.H., Fereidouni, M., Sedghiyan, D., Habibi, M. and Jung, D.W., 2021. Three-dimensional frequency response of the CNT-Carbon-Fiber reinforced laminated circular/annular plates under initially stresses. *Composite Structures*, *257*, pp.113146.

[63] Al-Furjan, M.S.H., Habibi, M., Ghabussi, A., Safarpour, H., Safarpour, M. and Tounsi, A., 2021. Non-polynomial framework for stress and strain response of the FG-GPLRC disk using three-dimensional refined higher-order theory. *Engineering Structures*, *228*, pp.111496.

[64] Dai, Z., Jiang, Z., Zhang, L. and Habibi, M., 2021. Frequency characteristics and sensitivity analysis of a size-dependent laminated nanoshell. *Advances in Nano Research*, *10*(2), pp.175-189.

[65] Wang, Z., Yu, S., Xiao, Z. and Habibi, M., 2020. Frequency and buckling responses of a high-speed rotating fiber metal laminated cantilevered microdisk. *Mechanics of Advanced Materials and Structures*. https://doi.org/10.1080/15376494.2020.1824284

[66] Ghabussi, A., Asgari Marnani, J. and Sadegh Rohanimanesh, M., 2021. Seismic performance assessment of a novel ductile steel braced frame equipped with steel curved damper. *Structures*, *31*, pp.87-97.

[67] Ghabussi, A., Habibi, M., Shavalipour, A., Moayedi, H., Safarpour, H. and Noormohammadi O., 2020. Frequency characteristics of a viscoelastic

graphene nanoplatelet–reinforced composite circular microplate. *Journal of Vibration and Control*, *27*, 107754632092393.

[68] Ghabussi, A., Asgari Marnani, J. and Sadegh Rohanimanesh, M., 2020. Improving seismic performance of portal frame structures with steel curved dampers. *Structures*, *24*, pp.27-40.

[69] Zhao, Y., Moradi, Z., Davoudi, M. and Zhuang, J., 2021. Bending and stress responses of the hybrid axisymmetric system via state-space method and 3D-elasticity theory. *Engineering with Computers*. https://doi.org/10.1007/s00366-020-01242-1

[70] Ma, L., Liu, X. and Moradi, Z., 2021. On the chaotic behavior of graphene-reinforced annular systems under harmonic excitation. *Engineering with Computers*. https://doi.org/10.1007/s00366-020-01210-9

[71] Jiao, J., Ghoreishi, S.M., Moradi, Z. and Oslub, K., 2021. Coupled particle swarm optimization method with genetic algorithm for the static–dynamic performance of the magneto-electro-elastic nanosystem. *Engineering with Computers*. https://doi.org/10.1007/s00366-021-01391-x

[72] Huang, X., Zhang, Y., Moradi, Z. and Shafiei, N., 2021. Computer simulation via a couple of homotopy perturbation methods and the generalized differential quadrature method for nonlinear vibration of functionally graded non-uniform microtube. *Engineering with Computers*. https://doi.org/10.1007/s00366-021-01395-7